

ORIGINAL ARTICLE

# ATM mediates constitutive NF- $\kappa$ B activation in high-risk myelodysplastic syndrome and acute myeloid leukemia

J Grosjean-Raillard<sup>1,2,3</sup>, M Tailler<sup>1,2,3</sup>, L Adès<sup>1,2,3,4</sup>, J-L Perfettini<sup>1,2,3</sup>, C Fabre<sup>1,2,3</sup>, T Braun<sup>4</sup>, S De Botton<sup>2</sup>, P Fenaux<sup>1,2,3,4</sup> and G Kroemer<sup>1,2,3</sup>

<sup>1</sup>INSERM U848, Institut Gustave Roussy, Villejuif, France; <sup>2</sup>Institut Gustave Roussy, Villejuif, France; <sup>3</sup>Université Paris Sud, Villejuif, France and <sup>4</sup>Service d'Hématologie Clinique, Hôpital Avicenne, AP-HP, Université Paris XIII, Bobigny, France

The anti-apoptotic transcription factor nuclear factor- $\kappa$ B (NF- $\kappa$ B) is constitutively activated in CD34<sup>+</sup> myeloblasts from high-risk myelodysplastic syndrome (MDS) and acute myeloid leukemia (AML) patients. Inhibition of NF- $\kappa$ B by suppressing the canonical NF- $\kappa$ B activation pathway, for instance by knockdown of the three subunits of the inhibitor of NF- $\kappa$ B (I $\kappa$ B) kinase (IKK) complex (IKK1, IKK2 and NEMO) triggers apoptosis in such cells. Here, we show that an MDS/AML model cell line exhibits a constitutive interaction, within the nucleus, of activated, S1981-phosphorylated ataxia telangiectasia mutated (ATM) with NEMO. Inhibition of ATM with two distinct pharmacological inhibitors suppressed the activating autophosphorylation of ATM, blocked the interaction of ATM and NEMO, delocalized NEMO as well as another putative NF- $\kappa$ B activator, PIDD, from the nucleus, abolished the activating phosphorylation of the catalytic proteins of the IKK complex (IKK1/2 on serines 176/180), enhanced the expression of I $\kappa$ B $\alpha$  and caused the relocalization of NF- $\kappa$ B from the nucleus to the cytoplasm, followed by apoptosis. Knockdown of ATM with small-interfering RNAs had a similar effect that could not be enhanced by knockdown of NEMO, PIDD and the p65 NF- $\kappa$ B subunit, suggesting that an ATM inhibition/depletion truly induced apoptosis through inhibition of the NF- $\kappa$ B system. Pharmacological inhibition of ATM also induced the nucleocytoplasmic relocalization of p65 in malignant myeloblasts purified from patients with high-risk MDS or AML, correlating with the induction of apoptosis. Altogether, these results support the contention that constitutively active ATM accounts for the activation of NF- $\kappa$ B in high-risk MDS and AML.

*Oncogene* (2009) 28, 1099–1109; doi:10.1038/onc.2008.457; published online 15 December 2008

**Keywords:** myelodysplastic syndrome; acute myeloid leukemia; ATM; NF- $\kappa$ B; IKK

## Introduction

Myelodysplastic syndromes (MDS) are clonal hematopoietic stem cell disorders characterized by ineffective hematopoiesis leading to blood cytopenias, especially anemia, and often evolving to acute myeloid leukemia (AML). MDS are relatively frequent diseases (incidence of 3–5 of 100 000 people per year) that largely predominate in the elderly (median age 65–70; Mufti *et al.*, 2003).

Myelodysplastic syndromes are classified based on morphology and blast cell percentage in blood and bone marrow (BM; French American British (FAB) and World Health Organization (WHO) classifications; Bennett *et al.*, 1976; Bennett, 2000). Main prognostic factors of MDS, for progression to AML and survival, include the number of cytopenias, the percentage of BM blasts and cytogenetic abnormalities. Those factors are combined in an International Prognostic Scoring System (IPSS) that distinguishes four subgroups with significantly different risk of progression to AML and survival: low, intermediate-1 (int-1); high, intermediate-2 (int-2). Low and int-1 subgroups are often grouped together as 'favorable' or lower risk MDS, and int-2 and high subgroups are 'unfavorable' or higher risk MDS (Greenberg *et al.*, 1997).

In low-risk MDS, the hypercellular BM is characterized by a grossly enhanced apoptotic turnover. In contrast, in high-risk MDS, apoptosis is suppressed because of a variety of factors including the constitutive activation of nuclear factor- $\kappa$ B (NF- $\kappa$ B) in malignant myeloblasts (Braun *et al.*, 2006b; Carvalho *et al.*, 2007). NF- $\kappa$ B acts as a mitogenic, anti-apoptotic transcription factor, and its inhibition kills high-risk MDS myeloblasts (Guzman *et al.*, 2001; Birkenkamp *et al.*, 2004), which hence are 'addicted' to NF- $\kappa$ B. High-risk MDS eventually transform into AML, in which marrow and circulating leukemic cells are 'addicted' to NF- $\kappa$ B as well (Guzman *et al.*, 2001; Birkenkamp *et al.*, 2004).

Nuclear factor- $\kappa$ B activation depends on phosphorylation and degradation of inhibitor proteins collectively termed I $\kappa$ B, which sequester NF- $\kappa$ B in the cytoplasm. Stimulation of the NF- $\kappa$ B pathway leads to the rapid phosphorylation of I $\kappa$ Bs and its subsequent

Correspondence: Dr G Kroemer, INSERM U848, Institut Gustave Roussy, Pavillon de Recherche 1, 39 rue Camille Desmoulins, Villejuif F-94805, France.

E-mail: kroemer@igr.fr

Received 10 June 2008; revised 21 October 2008; accepted 31 October 2008; published online 15 December 2008

degradation, resulting in NF- $\kappa$ B translocation into the nucleus. The phosphorylation of I $\kappa$ B $\alpha$  on serine residues 32 and 36 is initiated by an inhibitor of NF- $\kappa$ B kinase (IKK) complex which, at least in the canonical NF- $\kappa$ B activation pathway, includes a catalytic heterocomplex composed of IKK-1, IKK-2 and NEMO (Ghosh and Karin, 2002; Bonizzi and Karin, 2004; Greten and Karin, 2004). This pathway is activated in high-risk MDS and AML cells because chemical inhibition of IKK, knockdown of each of the components of the IKK complex (IKK1, IKK2, NEMO), inhibition of the proteasome (which is required for I $\kappa$ B degradation) or knockdown of p65 (the most abundant subunit of NF- $\kappa$ B) invariably interrupts anti-apoptotic NF- $\kappa$ B signaling and hence activates the apoptotic pathway (Campbell *et al.*, 2004; Karin *et al.*, 2004; Rajkumar *et al.*, 2005).

When mammalian cells are subjected to genetic damage, they undergo either repair for survival (often after a transient blockade of cell-cycle advancement) or enter the apoptotic default pathway. In this context, NF- $\kappa$ B can determine the 'existential choice' of DNA-damaged cells. DNA damage and in particular double-strand breaks result in the activation of ataxia telangiectasia mutated (ATM), a nuclear kinase that is required for NF- $\kappa$ B activation in response to many DNA-damaging agents (Li *et al.*, 2001; Huang *et al.*, 2003). ATM is also important for the regulation of cell-cycle checkpoints, DNA repair and apoptosis in the face of double-strand breaks (Bakkenist and Kastan, 2004). It has recently been reported that NEMO, the regulatory subunit of the IKK that is essential for NF- $\kappa$ B activation by DNA-damaging agents, underwent sequential modifications to enter into and exit the nucleus to ultimately permit IKK-mediated NF- $\kappa$ B activation (Li *et al.*, 2001; Huang *et al.*, 2003). This pathway of NF- $\kappa$ B activation appears to be uniformly induced by different anticancer treatments (Li *et al.*, 2001; Huang *et al.*, 2003). Nuclear NEMO forms a stable complex with activated ATM and is exported to the cytoplasm to activate the IKK complex. This in turn allows NF- $\kappa$ B to enter the nucleus and turn on genes important for cell survival (Huang *et al.*, 2003). Another NF- $\kappa$ B-activating protein that may be activated by DNA damage is PIDD, a protein that was originally identified as a p53-inducible gene (Lin *et al.*, 2000a) that can initiate apoptosis by caspase-2 activation (Tinel and Tschopp, 2004) and that can promote activation of IKK through a pathway that is not entirely elucidated (Janssens *et al.*, 2005). Hence, DNA damage can stimulate NF- $\kappa$ B activation through several pathways that involve a variable contribution of ATM and PIDD.

One of the main goals of our research is to decipher the constitutive activation of the NF- $\kappa$ B pathway in high-risk MDS and AML. Here, we show that ATM activates NF- $\kappa$ B in high-risk MDS and AML and that pharmacological inhibition of ATM induces apoptosis in malignant myeloblasts that are freshly isolated from the BM of high-risk MDS and AML patients.

## Results

### *ATM-dependent NF- $\kappa$ B activation induced by DNA damage in KG1 AML cells*

We chose to investigate the effect of DNA damage in KG1 AML cells, which do not exhibit constitutive NF- $\kappa$ B activation. KG1 cells were treated for 1 h with or without 100  $\mu$ M H<sub>2</sub>O<sub>2</sub>, a well-known donor of reactive oxygen species that can induce DNA damage (Barzilai and Yamamoto, 2004). Then the cells were rinsed and cultured in fresh medium. Following an overnight incubation, KG1 cells were then cultured for 2 h in the absence or presence of two ATM inhibitors (ATMIs), namely ATMI and KU55933. H<sub>2</sub>O<sub>2</sub> treatment induced NF- $\kappa$ B activation, as indicated by immunofluorescence detection of the NF- $\kappa$ B p65 subunit in the nucleus (Figure 1a). This H<sub>2</sub>O<sub>2</sub>-induced translocation of p65 from the cytoplasm to the nucleus was inhibited by both ATMIs. p65 also translocated into the nuclei of KG1 cells treated with two distinct DNA-damaging agents, ultraviolet C light or doxorubicin, and this effect was inhibited by ATMI or KU55933 (Figure 1b). Electrophoretic mobility shift assays (EMSAs) confirmed NF- $\kappa$ B activation by H<sub>2</sub>O<sub>2</sub> treatment and its inhibition by either one of the two ATMIs (Figure 1c). In addition, ATMI or KU55933 abolished the H<sub>2</sub>O<sub>2</sub>-induced phosphorylation of the IKK subunits 1/2 (IKK1/2), as determined in immunoblots using a phospho-neoepitope-specific antibody. ATMIs also enhanced the abundance of the IKK substrate, inhibitor of NF- $\kappa$ B $\alpha$  (I $\kappa$ B $\alpha$ ; Figure 1d). The H<sub>2</sub>O<sub>2</sub> and ATMI-mediated modulation of IKK1/2 phosphorylation and I $\kappa$ B $\alpha$  degradation were rapid phenomena, and could be observed within an incubation period as short as 1–2 h (Figure 1d).

In conclusion, in KG1 AML cells, distinct types of DNA damage can induce an ATM-dependent NF- $\kappa$ B activation that follows the canonical IKK1/2- and I $\kappa$ B $\alpha$ -dependent pathway.

### *ATM inhibition downregulates NF- $\kappa$ B and induces apoptosis in the MDS/AML cell line P39*

The presence of activated, phosphorylated ATM (on serine 1981) was monitored in four different AML cell lines, KG1 (which normally does not harbor constitutive NF- $\kappa$ B activity), MOLM-13, MV4-11 and P39 (which all exhibit constitutive NF- $\kappa$ B activation; Braun *et al.*, 2006a; Fabre *et al.*, 2007). Only P39 cells exhibited a strong constitutive ATM phosphorylation, which could be inhibited by ATMI or KU55933 (Figures 2a and b). ATMIs reduced NF- $\kappa$ B activation in P39 cells, as detected by EMSAs (Figure 2c). This effect was accompanied by a reduction of IKK1/2 phosphorylation and an increase in I $\kappa$ B $\alpha$  expression (Figure 2d). These effects of ATMI and KU55933 on P39 cells were obtained after an incubation period as short as 1–2 h. We found that nuclei from P39 cells also contained, in addition to p65 (Figure 2e), the IKK subunit NEMO (Figure 2f) as well as PIDD (Figure 2g), which is two proteins that have previously been reported to interact

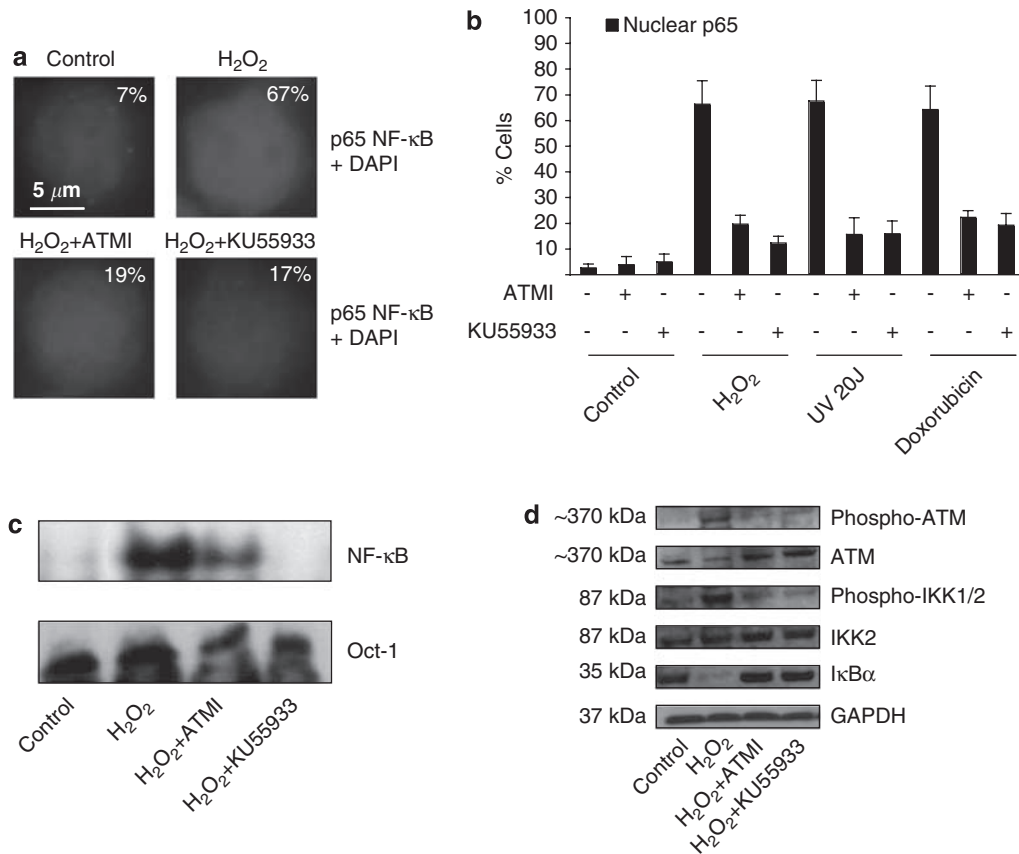


**Figure 1** Effects of DNA damage and ataxia telangiectasia mutated (ATM) inhibition on nuclear factor-κB (NF-κB) activation in KG1 cells. KG1 cells were treated for 1 h with 100 μM H<sub>2</sub>O<sub>2</sub>, washed and reincubated in normal growth medium overnight. Cells were then incubated in the absence or presence of ATM inhibitors (ATMIs; 10 μM) or KU55933 (10 μM) for 2 h and the nuclear localization of NF-κB was determined by immunofluorescence detection of p65 (**a**, **b**) and by electrophoretic mobility shift assay (EMSA) (**c**). Inhibitor of NF-κB kinase (IKK) 1/2 phosphorylation (serines 176 or 180) and IκB kinaseα (IκBα) degradation was assessed by immunoblot (**d**). Alternatively, KG1 cells were treated with 20 J of ultraviolet C (UVC) light or 25 nM doxorubicin and cultured overnight. Cells were then incubated in the absence or presence of ATMIs (10 μM) or KU55933 (10 μM), and the nuclear localization of NF-κB was assessed by immunofluorescence detection of p65 (**b**). These experiments were repeated three times, yielding similar results.

with ATM (Huang *et al.*, 2003; Habraken and Piette, 2006) and to shuttle between the nucleus and the cytoplasm (Janssens *et al.*, 2005; Habraken and Piette, 2006; Wu *et al.*, 2006). Of note, upon addition of either of the two ATMIs, p65, NEMO and PIDD moved from the nucleus to the cytoplasm (Figures 2e–h). Immunoprecipitation experiments revealed that in untreated P39 cells ATM and NEMO coimmunoprecipitate. This interaction was lost after treatment with ATMI or KU55933 (Figure 2i).

P39 cells exhibit constitutive activation of the NF-κB pathway, and inhibition of NF-κB kills these cells efficiently (Braun *et al.*, 2006a). As ATMIs suppress the NF-κB pathway in these cells, they should induce apoptosis. Accordingly, overnight incubation of P39 cells with ATMI- or KU55933-induced signs of apoptosis such as dissipation of the mitochondrial transmembrane potential ( $\Delta\Psi_m$ , determined by staining with the  $\Delta\Psi_m$ -sensitive fluorochrome DiOC<sub>6</sub>(3)), a subsequent loss of viability (determined with the vital dye propidium iodide, PI; Figures 3a and b), as well as DNA degradation leading to the accumulation of cells with a subdiploid DNA content (Figure 3c). This proapoptotic

effect of ATMIs was specific for P39 (not for MOLM-13, MV4-11 and KG1) cells (Figure 3b).

In conclusion, pharmacological ATMIs suppress the constitutive interaction between ATM and NEMO within the nuclei of P39 cells, reduce the constitutive phosphorylation of IKK1/2, enhance the abundance of IκBα, translocate the p65 NF-κB subunit from the nucleus to the cytoplasm and finally kill the cells.

*ATM knockdown inhibits NF-κB activation in P39 cells*  
As chemical inhibitors of tyrosine kinases often (if not always) inhibit other targets than the kinase that they had originally been designed for, we attempted to exclude possible off-target effects of ATMIs by an alternative strategy of ATM inhibition. Knockdown of ATM with two distinct-specific small-interfering RNAs (siRNAs, which was maximal 48 h after transfection) reduced the phosphorylation of IKK1/2 and increased the abundance of IκBα (Figure 4a), as well as that of EMSA-detectable NF-κB in the nucleus (Figure 4b). Similarly, ATM knockdown led to the depletion of

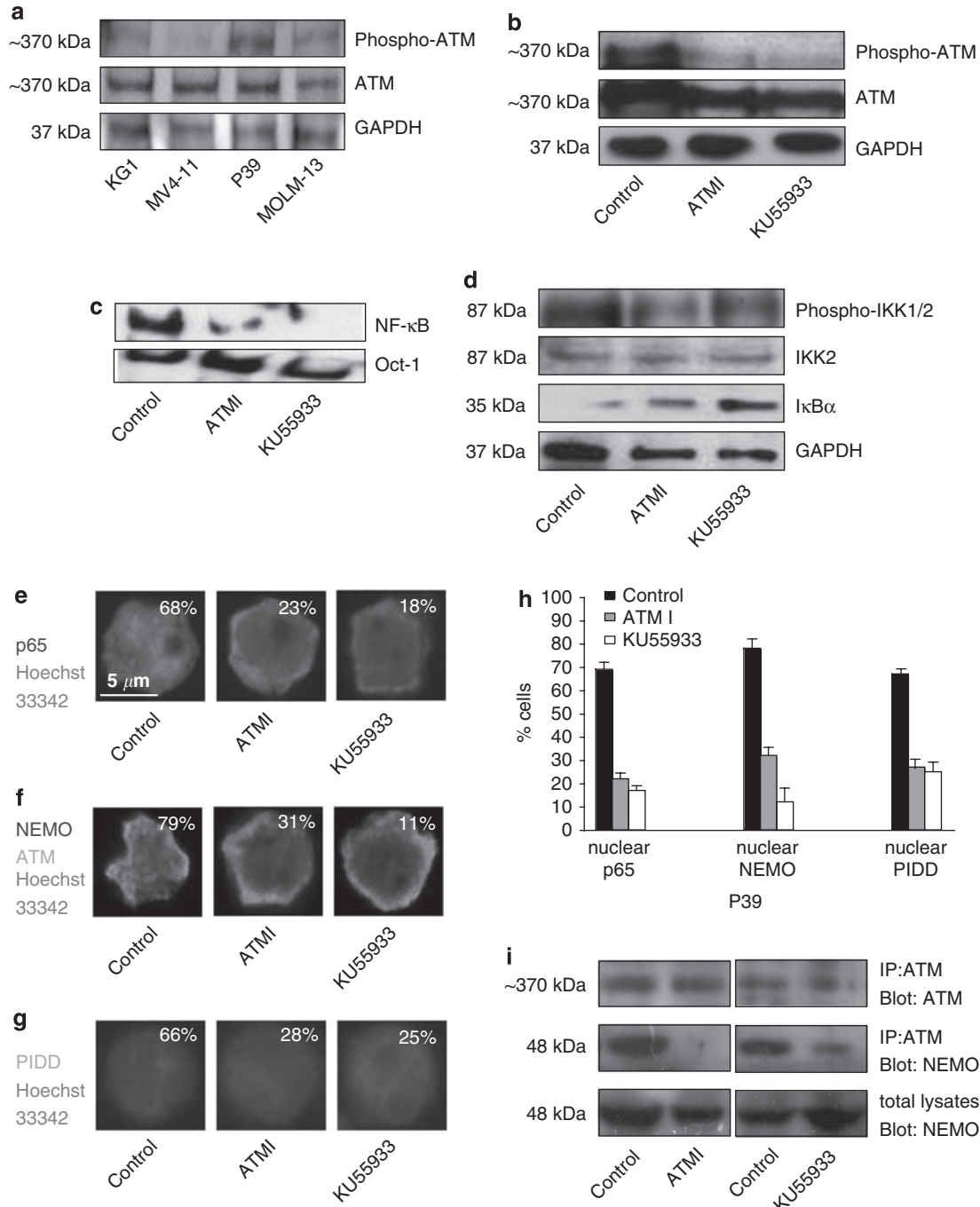


**Figure 2** Effect of ataxia telangiectasia mutated (ATM) inhibition (ATMI) on the nuclear factor- $\kappa$ B (NF- $\kappa$ B) system in P39 cells. Immunoblot detection of ATM and its activating phosphorylation in different cell lines (**a**, **b**). Extracts from the indicated cell lines were subjected to SDS/polyacrylamide gel electrophoresis (PAGE) and immunoblot detection of phosphorylated ATM, ATM protein irrespective of the phosphorylation status or glyceraldehyde-3-phosphate dehydrogenase (GAPDH) as a loading control. P39 cells were treated or not with the ATMIs (10  $\mu$ M) or KU55933 (10  $\mu$ M) for 2 h before lysis (**b**). Electrophoretic mobility shift assay (EMSA) detection of nuclear factor- $\kappa$ B (NF- $\kappa$ B) in nuclear extracts from untreated P39 cells or cells treated with ATMI or KU55933 (10  $\mu$ M both, for 2 h) (**c**). Immunoblot detection of inhibitor of NF- $\kappa$ B kinase (IKK) 1/2 phosphorylation and I $\kappa$ B $\alpha$  degradation after addition of ATMI or KU55933 to P39 cells (**d**). Subcellular redistribution of ATM, NEMO and PIDD after ATMI (**e**–**g**). P39 cells were either left untreated (control) or cultured in the presence of ATMI (10  $\mu$ M) or KU55933 (10  $\mu$ M) for 2 h and then fixed, permeabilized and subjected to two-color immunofluorescence staining for the simultaneous detection of p65 and chromatin (Hoechst 33342) (**e**), ATM and NEMO (**f**) or PIDD and chromatin (**g**). Individual cells representative of >90% of the dominant phenotype are shown. Histograms represent means  $\pm$  s.d. of triplicates (**h**). All experiments were repeated at least three times, yielding similar results. Effect of ATMIs on the nuclear interaction between ATM and NEMO (**i**). P39 cells were left untreated or were treated with ATMI (10  $\mu$ M) or KU55933 (10  $\mu$ M) for 2 h, followed by immunoprecipitation of ATM and detection of NEMO (**i**).

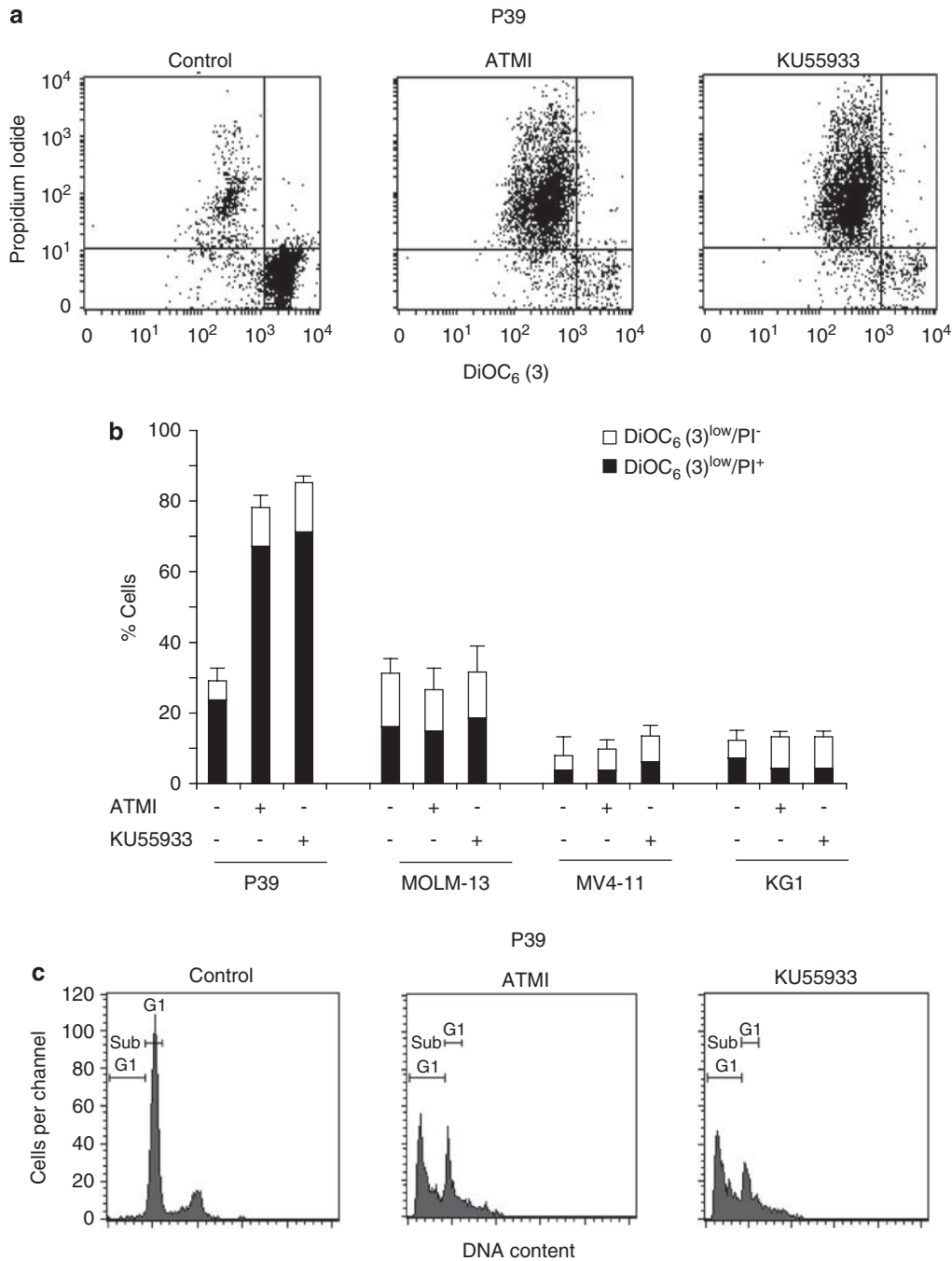


**Figure 3** Apoptosis induction by ataxia telangiectasia mutated (ATM) inhibition (ATMI) in P39 cells. Detection of mitochondrial signs of apoptosis after treatment with ATMI (a). P39 cells were cultured in the absence or presence of ATMI (50  $\mu$ M) or KU55933 (50  $\mu$ M) for 18 h and then stained with the  $\Delta\Psi_m$ -sensitive dye DiOC<sub>6</sub>(3) and the vital dye propidium iodide (PI), followed by cytofluorometric analysis. Representative quantitative data ( $\bar{X} \pm$  s.d. of triplicates) are shown in (b) for P39, MOLM-13, MV4-11 and KG1 cells. Detection of apoptotic DNA loss after ATMI (50  $\mu$ M, 18 h). P39 cells were ethanol-fixed, treated with RNase, labeled with PI and subjected to cell-cycle analysis. Results are typical for three independent experiments (c).

immunofluorescence-detectable p65 from the nucleus (Figure 4c). In addition, ATM depletion caused cell death, as indicated by the loss of  $\Delta\Psi_m$  and plasma membrane integrity. This proapoptotic effect of ATM knockdown could not be further enhanced by depleting p65, NEMO or PIDD with two confirmed siRNAs each

(Lin *et al.*, 2000b; Braun *et al.*, 2006a; Carvalho *et al.*, 2007; Figure 4d). This kind of epistatic analysis confirms that ATM is required for the constitutive activation of NF- $\kappa$ B in P39 cells and suggests that the proapoptotic effect of ATM depletion is mediated through NF- $\kappa$ B inactivation.

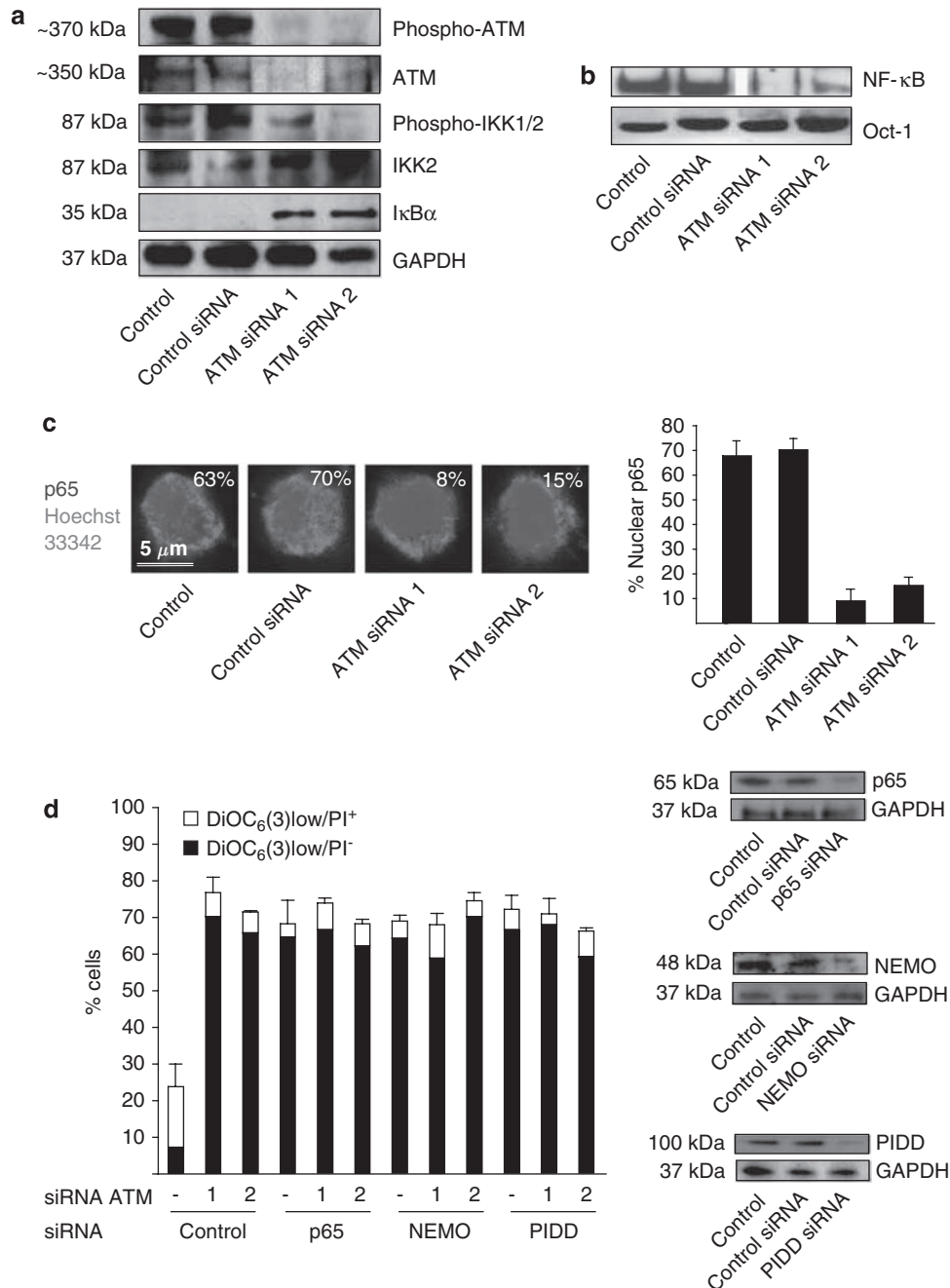


**Figure 4** Knockdown of ataxia telangiectasia mutated (ATM) causes nuclear factor- $\kappa$ B (NF- $\kappa$ B) inhibition and apoptosis of P39 cells. P39 cells were electroporated with two small-interfering RNAs (siRNAs) specific for ATM, and the expression level and phosphorylation status of ATM, inhibitor of nuclear factor- $\kappa$ B (NF- $\kappa$ B) kinase (IKK) 1/2 and degradation of inhibitor of NF- $\kappa$ B $\alpha$  (I $\kappa$ B $\alpha$ ) were detected by immunoblot 48 h later (**a**). NF- $\kappa$ B activation was measured by electrophoretic mobility shift assay (EMSA) (**b**), or immunofluorescence detection of the p65 NF- $\kappa$ B subunit (**c**), and the frequency of dying cells ( $X \pm$  s.d.,  $n = 3$ ) was determined by DiOC<sub>6</sub>(3)/PI staining (**d**). The blots in (**d**) illustrate the depletion of p65, NEMO or PIDD after transfection with specific siRNAs. This experiment has been repeated three times, with similar results.

#### Ex vivo effects of ATM inhibition on primary MDS and AML cells

Apoptosis induction by ATMIs has been observed with one single cell line and hence these data must be interpreted with caution as to their possible clinical relevance. We therefore studied the impact of the two specific ATMIs ATMI and KU55933, on primary,

purified CD34<sup>+</sup> BM mononuclear cells (BM-MNCs) from a cohort of MDS and AML patients (Table 1). CD34<sup>+</sup> BM-MNC from donors healthy contained less than 1% of cells that stained positively for phospho-ATM, in agreement with the previously reported low index of normal BM cells with phospho-ATM (Bartkova *et al.*, 2005a). In contrast, in all patients (that is in 10 out

**Table 1** Characteristics of MDS patients

Number	Age	Karyotype	Disease	IPSS	% Bone marrow blasts	% Phospho-ATM positive	% Nuclear p65	% Nuclear p65 after ATMI treatment	% Nuclear p65 after KU55933 treatment
1	62	46,XX	Control	NA	0	0	5	4	11
2	80	46,XY	Control		0	0	7	5	13
3	63	46,XX	Control		0	0	10	10	10
4	84	46,XX del(20q)	Pure RA	Low	1	2	12	11	11
5	68	46,XX	RCMD	Low	1	0	17	15	15
6	84	46,XY	RCMD	Low	1	5	25	20	18
7	85	46,XY	Pure RA	Int-1	1	0	22	19	21
8	68	46,XX +8	RAEB-1	Int-1	7	13	38	12	11
9	85	46,XX del(11q)	RAEB-1	Int-2	8	15	25	15	13
10	72	46,XX	RAEB-2	Int-2	15	12	37	14	14
11	82	46,XX	RAEB-2	Int-2	15	11	28	9	5
12	74	46,XY	RAEB-2	Int-2	14	11	22	8	6
13	87	46,XX +8	RAEB-1	Int-2	6	16	42	21	17
14	77	46,XY	RAEB-2	Int-2	16	43	31	10	11
15	66	46,XY complex	CMML	Int-2	10	70	42	11	9
16	72	46,XY	CMML	Int-2	15	55	40	6	10
17	78	46,XX	RAEB-2	Int-2	14	91	60	7	9
18	37	46,XY inv(16)	AML	ND	46	50	40	5	6
19	86	46,XX	AML	ND	57	78	67	12	10
20	68	46,XX	AML	ND	70	67	81	13	9

Abbreviations: AML, acute myeloid leukemia; ATM, ataxia telangiectasia mutated; ATMI, ATM inhibitor; CMML, chronic myelomonocytic leukemia; complex, complex karyotype was defined as three or more cytogenetic abnormalities; del, deletion; inv, inversion; IPSS, International Prognostic Scoring System; MDS, myelodysplastic syndrome; NA, not applicable; ND, not determined; RA, refractory anemia; RAEB, refractory anemia with excess of blasts (5–9% BM blasts: RAEB-1; 10–19% BM blasts: RAEB-2); RARS, RA with ringed sideroblasts; RCMD, refractory cytopenia with multilineage dysplasia; sAML, secondary AML.

of 10) with high-risk MDS or AML, a substantial fraction (20–90%) of CD34<sup>+</sup> BM-MNC stained positively for phospho-ATM, whereas patients with low-risk MDS were heterogeneous with respect to phospho-ATM staining (Table 1). This finding is reminiscent of the finding that high-risk lesions of several types of solid tumors also exhibit cells with phosphorylated ATM (Bartkova *et al.*, 2005b). CD34<sup>+</sup> cells from normal donors or patients were cultured either alone or in the presence of ATMI or KU55933 for 18 h *ex vivo*, followed by assessment of their spontaneous and ATM inhibition-induced mortality. As depicted in Figures 5a and b, ATMIs had no significant cytotoxic effects on CD34<sup>+</sup> BM cells from three distinct healthy donors (Figures 5a and b). As reported (Guzman *et al.*, 2001; Birkenkamp *et al.*, 2004), CD34<sup>+</sup> BM cells from low-risk MDS patients succumbed to apoptosis spontaneously, and this enhanced baseline mortality was not accelerated by ATMIs (Figures 5a and b). In contrast, CD34<sup>+</sup> BM cells from high-risk MDS patients and AML patients exhibited a significant ( $P < 0.01$ , paired Student's *t*-test) apoptotic response to ATMIs (Figures 5a and b). Next, we assessed parameters of NF- $\kappa$ B inhibition in several AML and high-risk MDS patients whose CD34<sup>+</sup> BM cells responded to both ATMIs *ex vivo* (Figures 5c and d). For both AML and high-risk MDS patients, we found that ATM inhibition reduced the constitutive activation of NF- $\kappa$ B, as indicated by a loss of the nuclear p65 immunofluorescence staining (Figures 5c and d).

Chemical inhibition of ATM caused an inhibition of NF- $\kappa$ B as seen by EMSAs (Figure 6a) and by immunofluorescence analyses (Figure 6b) of CD34<sup>+</sup> BM cells from AML and high-risk MDS patients. This was accompanied by the redistribution of NEMO from a nuclear to a cytoplasmic localization (Figure 6c), exactly as we had observed in P39 cells (Figure 2f). Furthermore, after addition of ATMI or KU55933, PIDD translocated from the nucleus to the cytoplasm (Figure 6b). This result was obtained on CD34<sup>+</sup> BM myeloblasts from several AML and high-risk MDS patients, and representative data are shown for one representative AML patient (patient 17 in Table 1).

Altogether, these data allow us to draw two major conclusions. First, constitutive NF- $\kappa$ B activation in high-risk MDS and AML correlated with constitutive ATM phosphorylation and activation. Second, inhibition of ATM reduces this malignancy-associated NF- $\kappa$ B activation, presumably through the same pathway that has been delineated for P39 cell lines.

#### Concluding remarks

The results presented in this study indicate that ATM may act as a possible upstream kinase that mediated constitutive NF- $\kappa$ B activation in marrow blasts in high-risk MDS and AML. This notion is based on the comparative analysis of ATM inhibition (either by means of a pharmacological inhibitors or using distinct

siRNAs) in P39 MDS/AML cells or patient-derived, CD34<sup>+</sup> primary BM cells.

Our data are compatible with the following scenario. ATM is constitutively phosphorylated and active in malignant myeloblasts, as represented by P39 cells, perhaps as a result of cancer-associated genomic instability (Halazonetis *et al.*, 2008). Active ATM interacts with NEMO (and likewise with PIDD) in the nucleus, presumably causing the activation of NEMO and that of the other proteins of the IKK complex, IKK1 and 2, which exhibit an activating phosphorylation. The IKK complex causes the phosphorylation and hence degradation of I $\kappa$ B $\alpha$ , thereby facilitating the translocation of NF- $\kappa$ B into the nucleus and activation of an anti-apoptotic transcriptional program. When ATM is inhibited, its interaction with NEMO is lost. Unexpectedly, the ATM inhibition also causes the relocation of PIDD to the nucleus, in spite of the fact that both proteins have been reported to act independently of each other (Habraken and Piette, 2006). This points to the possibility that ATM inhibition might cause the inactivation of NEMO by two effects, one involving the interaction between ATM and NEMO and another

(independent?) one involving the nuclear release of PIDD. Irrespective of the exact molecular mechanism, ATM inhibition is coupled to the deactivation of the IKK complex (as indicated by the dephosphorylation of IKK1/2) and hence the stabilization of I $\kappa$ B $\alpha$ , resulting in the cytoplasmic sequestration of NF- $\kappa$ B and consequent deactivation of the NF- $\kappa$ B system. As P39 cells are 'addicted' to NF- $\kappa$ B, switching of the NF- $\kappa$ B system by ATM inhibition has fatal consequences and unleashes the mitochondrial pathway of apoptosis. Epistatic analyses suggest that p65, NEMO and PIDD act on the same pathway as ATM to maintain cellular viability, because the lethal effect of ATM depletion was not exacerbated by the removal of any among the three other proteins.

It should be noted that only one MDS/AML cell line (P39) among a panel of three cell lines that showed constitutive NF- $\kappa$ B activation (P39, MOLM-13 and MV4-11) exhibited ATM phosphorylation and responded to ATMI by inactivating NF- $\kappa$ B and by undergoing apoptosis. Indeed, the other two cell lines (MOLM-13 and MV4-11) exhibited the constitutive phosphorylation of the oncogenic receptor tyrosine

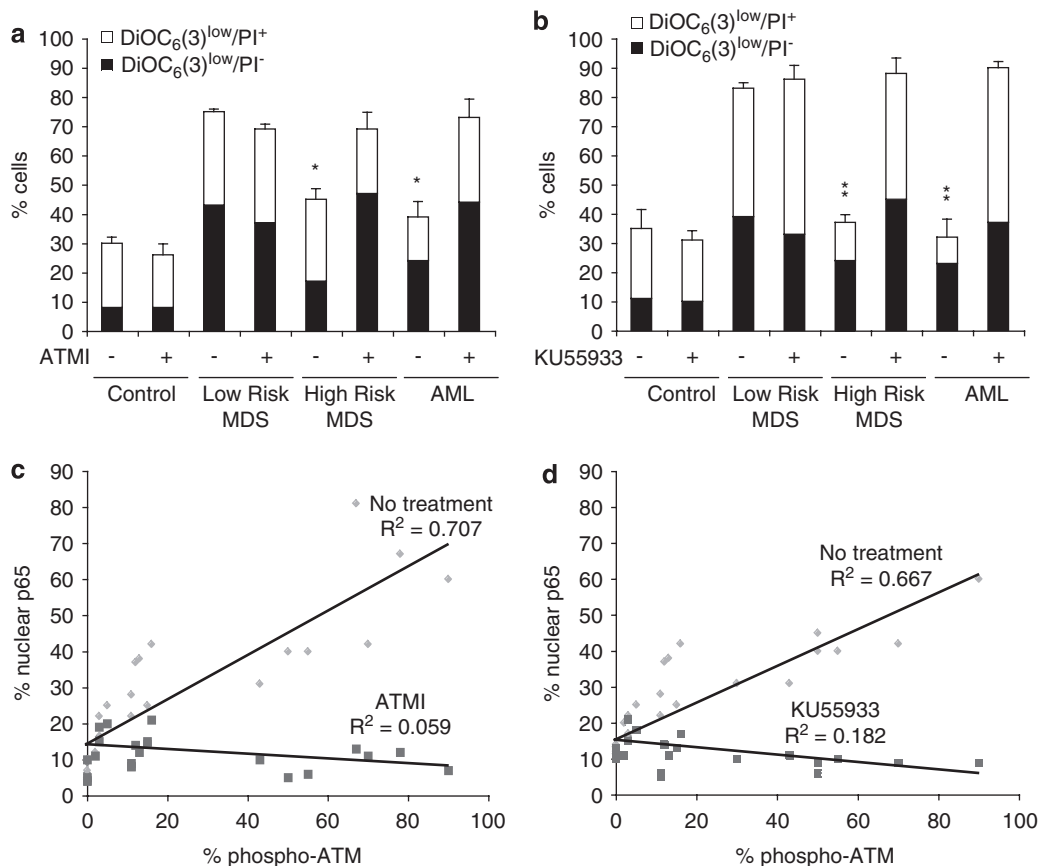


**Figure 5** Effect of ataxia telangiectasia mutated (ATM) inhibition (ATMI) on constitutive nuclear factor- $\kappa$ B (NF- $\kappa$ B) activation and cell death of purified CD34<sup>+</sup> bone marrow cells from myelodysplastic syndrome (MDS) and acute myeloid leukemia (AML) patients. Results of DiOC<sub>6</sub>(3)/PI stainings ( $\bar{X} \pm$  s.e.m.) of CD34<sup>+</sup> AML bone marrow cells cultured for 18 h in the absence or presence of ATMI (50  $\mu$ M) (a) or KU55933 (50  $\mu$ M) (b) as in Figures 3a and b. Statistical analyses (\* $<0.05$ ; \*\* $<0.01$ ) were performed by means of the paired Student's *t*-test. Correlation between the phosphorylation status of ATM and the subcellular localization of the p65 NF- $\kappa$ B subunit of CD34<sup>+</sup> AML bone marrow cells (same patient as in a and b), as determined by immunofluorescence, before and after treatment with ATMI (c) or KU55933 (d). Each dot represents values for one patient.

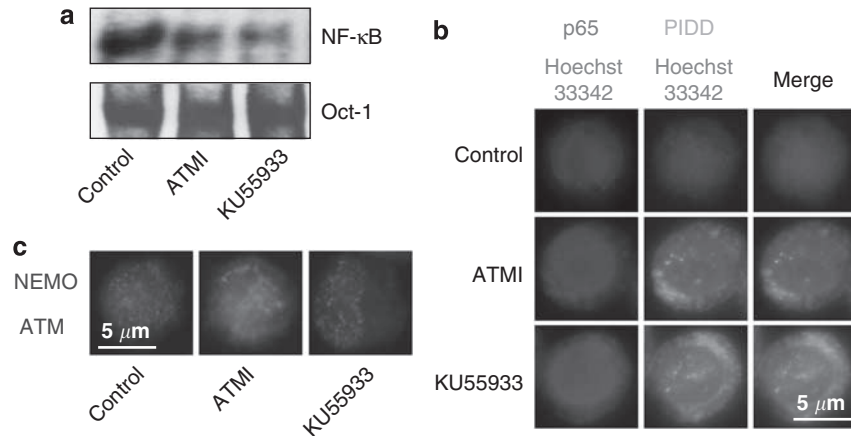


**Figure 6** Inhibition of nuclear factor- $\kappa$ B (NF- $\kappa$ B) activation in a representative acute myeloid leukemia (AML) patient. Nuclear NF- $\kappa$ B in the absence or in the presence of ataxia telangiectasia mutated (ATM) inhibitors (ATMIs), as determined by electrophoretic mobility shift assay (EMSA) (a). Effect of ATMIs or KU55933 (10  $\mu$ M, 2 h) on the subcellular localization of p65, ATM, NEMO and PIDD (b, c). Representative fluorescence microphotographs are shown. Similar results were obtained for three different AML and two different myelodysplastic syndrome (MDS) patients.

kinase Flt3 and activated NF- $\kappa$ B through activated Flt3, meaning that they readily succumbed upon pharmacological inhibition or depletion of Flt3 (Grosjean-Raillard *et al.*, 2008). In contrast, P39 cells whose NF- $\kappa$ B activation depends on ATM do not express Flt3 and are insensitive to Flt3 inhibitors (Grosjean-Raillard *et al.*, 2008). These observations point to the interesting possibility that different populations of malignant cells (which are represented by different cell lines) use distinct mechanisms for activating NF- $\kappa$ B. There is a considerable heterogeneity in the response of AML patients to Flt3 inhibitors (Yanada *et al.*, 2005; Knapper, 2007; Gale *et al.*, 2008) or ATMIs (this study), and it will be important to assess the combined proapoptotic effect of kinase inhibitors affecting Flt3 and ATM on preclinical models of AML in the future. Preliminary data obtained with purified CD34<sup>+</sup> BM cells from a limited number of patients suggest that there are two different groups of patients, one group whose marrow blasts respond preferentially to ATMIs and another group that preferentially responds to Flt3 inhibitors.

Irrespective of these details, our data suggest the intriguing possibility to kill malignant myeloblast by inhibiting (one of) the upstream kinase(s) that account for constitutive activation of the NF- $\kappa$ B pathway. Although other studies suggested that ATM might be used as a chemo- or radiosensitizing agents (Leone *et al.*, 2007), the result of our work implies that ATM inhibition as such could have a therapeutic effect on high-risk MDS and AML. This hypothesis warrants further preclinical and clinical exploration.

## Materials and methods

### Patients

Acute myeloid leukemia, MDS patients and healthy subjects were included in our study (Table 1). Informed consent of all patients and healthy subjects was provided according to the Declaration of Helsinki. This study was approved by the

Institut Gustave Roussy institutional review board. MDS patients were previously untreated except for supportive care. The diagnosis of MDS was based on peripheral blood counts, cytology of peripheral blood and BM according to the WHO classification (Vardiman *et al.*, 2002) and conventional cytogenetic analysis. These data evaluation of the individual IPSS score were assessed for each patient (Greenberg *et al.*, 1997). BM aspirates were collected after informed consent into syringes containing media supplemented with EDTA. The BM-MNC fraction was isolated by density gradient centrifugation using Ficoll-Paque Plus (Amersham Biosciences, Sunnyvale, CA, USA) and then washed three times (10 min, 600 g, 4 °C) in complete medium.

### Cells and culture conditions

Myelodysplastic syndrome -derived leukemia cell line P39/Tsugane was obtained from Professor Y Yoshida (Center for South East Asian Studies, Kyoto University, Kyoto, Japan) and KG1 were purchased from the Deutsche Sammlung von Mikroorganismen und Zellkulturen GmbH, Germany. All cell lines were cultured in Roswell Park Memorial Institute 1640 medium (Gibco, Carlsbad, CA, USA) supplemented with 10% heat-inactivated fetal calf serum (FCS), 2 mM L-glutamine, 100 IU/ml penicillin and 100  $\mu$ g/ml streptomycin as described (Hassan *et al.*, 1999). BM cells were isolated and processed as follows: after density gradient (Ficoll-Paque Plus) separation of BM-MNC, CD34<sup>+</sup> cells were isolated by positive selection with the MiniMacs system (Miltenyi Biotec, Bergisch Gladbach, Germany) and then maintained in Iscove's modified Dulbecco's medium (Gibco) supplemented with 10% heat-inactivated FCS. We used distinct inhibitors to suppress the ATM activity: ATMI purchased from Calbiochem (Darmstadt, Germany) (2-morpholin-4-yl-6-thianthren-1-yl-pyran-4-one), KU55933 (Hickson *et al.*, 2004) and doxorubicin (Sigma, St Louis, MO, USA).

### Transfection of plasmids and knockdown of ATM by siRNA

Cells were transfected with the Nucleofector system (Amaxa, Cologne, Germany) using siRNAs specific for GFP (5'-GCAAGCTGACCCTGAAGTTCA-3') with no homology to human genes (EGFP siRNA; InvivoGen/InvivoGen, San Diego, CA, USA), a pool of siRNAs specific for ATM, NEMO or p65 (Upstate, Lake Placid, NY, USA), validated ATM siRNAs (Qiagen, Valencia, CA, USA) and siRNAs

specific for PIDD (Santa Cruz Biotechnology, Santa Cruz, CA, USA). Cells were used 48 h after transfection.

#### Assessment of apoptosis

Cells ( $10^5$ ) from MDS and AML cell lines or patient cells were resuspended in 1 ml of culture medium and incubated in the presence or absence of 50  $\mu$ M ATMI peptide or 50  $\mu$ M of KU55933 for 48 h. Apoptotic cells were detected by flow cytometric analysis using a FACScan (Becton Dickinson, Mountain View, CA, USA), as described previously (Castedo *et al.*, 2002; Zamzami and Kroemer, 2004). Cells were stained with propidium iodide (PI, 10  $\mu$ M, Sigma, St Louis, MO, USA) and 20 nM fluorochrome DiOC<sub>6</sub>(3) (Molecular Probes, Eugene, OR, USA) for 15 min at 37 °C, for the determination of plasma membrane permeability and the mitochondrial transmembrane potential ( $\Delta\Psi_m$ ), respectively (Castedo *et al.*, 1996; Metivier *et al.*, 1998).

#### Nuclear protein extraction and electrophoretic mobility shift assay

Nuclear extracts were prepared from all cell lines after culture in the presence or absence of ATMIs (standard treatment: 10  $\mu$ M, 2 h). Cells were harvested and washed twice with ice-cold phosphate-buffered saline (PBS). Cell pellets were then lysed in hypotonic lysis buffer (10 mM *N*-2-hydroxyethylpiperazine-*N'*-2-ethanesulfonic acid-potassium hydroxide (HEPES), 1.5 mM MgCl<sub>2</sub>, 10 mM KCl and 0.0125% NP-40, pH 7.9). After incubation on ice for 10 min, nuclei were separated from the cytosolic extracts by centrifugation (13 000 *g* 5 min at 4 °C). The nuclear pellets were resuspended in hypertonic extraction buffer (5 mM HEPES, 1 mM MgCl<sub>2</sub>, 0.2 mM EDTA, 0.5 M NaCl, 25% glycerol and 0.025% NP-40, pH 7.0) for 30 min at 4 °C under agitation. After centrifugation at 13 000 *g* 15 min at 4 °C, supernatants containing nuclear proteins were removed and stored at -70 °C. Nuclear extracts were examined for NF- $\kappa$ B-binding activity by EMSA, using a nonradioactive EMSA kit (Panomics, Fremont, CA, USA).

#### Immunofluorescence stainings

Cell lines or patient cells ( $10^5$ ) were allowed to adhere to polylysine-L coverslips (Sigma) and fixed in PBS containing 4% paraformaldehyde at room temperature. Cells were then permeabilized either with 0.05% Triton X-100 (Boehringer, Mannheim, Germany) or 0.1% SDS for 10 min, washed in PBS and stained with antibodies specific for p65 (rabbit polyclonal Ab, Santa Cruz Biotechnology), PIDD (Santa Cruz Biotechnology), phospho-ATM (Upstate), NEMO (Santa Cruz Biotechnology) and revealed either with a goat anti-rabbit or a goat anti-goat IgG coupled with Alexa 568 (red) or Alexa 488 (green) fluorochromes (Molecular Probes). Nuclei were counterstained with DAPI or Hoechst 33342 (Molecular Probes), allowing for the discernment of chromatin condensation (Castedo *et al.*, 2002). A total of 200 cells for each slide were examined independently with a LSM 510 confocal microscope (Zeiss) at a 63-fold magnification.

#### Immunoblots

Cellular lysates (50  $\mu$ g protein per lane) were subjected to SDS/polyacrylamide gel electrophoresis, transferred on nitrocellu-

lose membranes and immunochemical detection was carried out using antibodies specific for I $\kappa$ B $\alpha$  (rabbit polyclonal Ab, Santa Cruz Biotechnology), phospho-IKK1-2 (Cell Signaling Technology, Boston, MA, USA), IKK1 (rabbit polyclonal Ab, Santa Cruz Biotechnology), IKK2 (rabbit polyclonal Ab, Santa Cruz Biotechnology), NEMO (rabbit polyclonal Ab, Santa Cruz Biotechnology) ATM (rabbit polyclonal Ab, Abcam, Cambridge, MA, USA), p65 (rabbit polyclonal Ab, Santa Cruz Biotechnology), PIDD (Santa Cruz Biotechnology), phospho-ATM (Upstate), NEMO (Santa Cruz Biotechnology) or glyceraldehyde-3-phosphate dehydrogenase (Abcam).

#### Immunoprecipitation

Following treatment, cells were lysed in RIPA buffer (50 mM Tris-HCl, pH 8, 150 mM NaCl, 1% NP-40, 0.5% sodium deoxycholate, 0.1% SDS) and 200  $\mu$ g were immunoprecipitated with the antibody of interest for 2 h and incubated with protein G-coupled sepharose beads (Roche Applied Science, Rockford, IL, USA) overnight at 4 °C. Immunoprecipitates were obtained following several centrifugation per wash cycles in lysis buffer followed by immunoblotting.

#### Abbreviations

AML, acute myeloid leukemia; BM-MNC, bone marrow mononuclear cells; DAPI, 4',6-diamidino-2-phenylindole; DiOC<sub>6</sub>(3), 3,3'-dihexyloxycarbocyanine iodide; I $\kappa$ B, inhibitor of NF- $\kappa$ B; IKK, I $\kappa$ B kinase; MDS, myelodysplastic syndrome; NF- $\kappa$ B, nuclear factor- $\kappa$ B; PI, propidium iodide.

#### Acknowledgements

We are indebted to Jalil Abdelali (Institut Gustave Roussy, Villejuif, France) for technical support in confocal microscopy. Guido Kroemer is supported by the Agence Nationale de Recherche, Fondation de France, Cent pour Sang la Vie, Cancéropôle Ile-de-France, Institut National du Cancer, Ligue Nationale contre le Cancer and the European Community (Active p53, Apo-Sy, Apop-Train, TransDeath, RIGHT, ChemoRes). Jennifer Grosjean received a postdoctoral fellowship by Cancéropôle Ile-de-France. Lionel Adès received a scholarship from Assistance Publique-Hopitaux de Paris and Caisse Nationale d'Assurance Maladie des Professions Indépendantes. Claire Fabre received a scholarship from Fondation pour la Recherche Médicale. Maximilien Tailler received a PhD fellowship from Université Paris Sud, Paris 11.

#### Author contributions

JG-R and MT performed the experiments and analysed the data. LA, CF, TB and SDB provided BM samples and essential clinical information on patients. AI and PF participated in the conception of the study. GK conceived and directed the study. JG-R and GK wrote the paper.

#### References

Bakkenist CJ, Kastan MB. (2004). Phosphatases join kinases in DNA-damage response pathways. *Trends Cell Biol* **14**: 339–341.  
Bartkova J, Bakkenist CJ, Rajpert-De Meyts E, Skakkebaek NE, Sehested M, Lukas J *et al.* (2005a). ATM activation in

normal human tissues and testicular cancer. *Cell Cycle* **4**: 838–845.  
Bartkova J, Horejsi Z, Koed K, Kramer A, Tort F, Zieger K *et al.* (2005b). DNA damage response as a candidate anti-cancer

- barrier in early human tumorigenesis. *Nature* **434**: 864–870.
- Barzilai A, Yamamoto K. (2004). DNA damage responses to oxidative stress. *DNA Repair (Amst)* **3**: 1109–1115.
- Bennett JM. (2000). World Health Organization classification of the acute leukemias and myelodysplastic syndrome. *Int J Hematol* **72**: 131–133.
- Bennett JM, Catovsky D, Daniel MT, Flandrin G, Galton DA, Gralnick HR *et al.* (1976). Proposals for the classification of the acute leukaemias. French–American–British (FAB) co-operative group. *Br J Haematol* **33**: 451–458.
- Birkenkamp KU, Geugien M, Schepers H, Westra J, Lemmink HH, Vellenga E. (2004). Constitutive NF-kappaB DNA-binding activity in AML is frequently mediated by a Ras/PI3-K/PKB-dependent pathway. *Leukemia* **18**: 103–112.
- Bonizzi G, Karin M. (2004). The two NF-kappaB activation pathways and their role in innate and adaptive immunity. *Trends Immunol* **25**: 280–288.
- Braun T, Carvalho G, Coquelle A, Vozenin MC, Lepelley P, Hirsch F *et al.* (2006a). NF-kappaB constitutes a potential therapeutic target in high-risk myelodysplastic syndrome. *Blood* **107**: 1156–1165.
- Braun T, Carvalho G, Fabre C, Grosjean J, Fenaux P, Kroemer G. (2006b). Targeting NF-kappaB in hematologic malignancies. *Cell Death Differ* **13**: 748–758.
- Campbell KJ, Rocha S, Perkins ND. (2004). Active repression of antiapoptotic gene expression by RelA(p65) NF-kappa B. *Mol Cell* **13**: 853–865.
- Carvalho G, Fabre C, Braun T, Grosjean J, Ades L, Agou F *et al.* (2007). Inhibition of NEMO, the regulatory subunit of the IKK complex, induces apoptosis in high-risk myelodysplastic syndrome and acute myeloid leukemia. *Oncogene* **26**: 2299–2307.
- Castedo M, Hirsch T, Susin SA, Zamzami N, Marchetti P, Macho A *et al.* (1996). Sequential acquisition of mitochondrial and plasma membrane alterations during early lymphocyte apoptosis. *J Immunol* **157**: 512–521.
- Castedo M, Perfettini JL, Kroemer G. (2002). Mitochondrial apoptosis and the peripheral benzodiazepine receptor: a novel target for viral and pharmacological manipulation. *J Exp Med* **196**: 1121–1125.
- Fabre C, Carvalho G, Tasdemir E, Braun T, Ades L, Grosjean J *et al.* (2007). NF-kappaB inhibition sensitizes to starvation-induced cell death in high-risk myelodysplastic syndrome and acute myeloid leukemia. *Oncogene* **26**: 4071–4083.
- Gale RE, Green C, Allen C, Mead AJ, Burnett AK, Hills RK *et al.* (2008). The impact of FLT3 internal tandem duplication mutant level, number, size, and interaction with NPM1 mutations in a large cohort of young adult patients with acute myeloid leukemia. *Blood* **111**: 2776–2784.
- Ghosh S, Karin M. (2002). Missing pieces in the NF-kappaB puzzle. *Cell* **109**(Suppl): S81–S96.
- Greenberg P, Cox C, LeBeau MM, Fenaux P, Morel P, Sanz G *et al.* (1997). International scoring system for evaluating prognosis in myelodysplastic syndromes. *Blood* **89**: 2079–2088.
- Greten FR, Karin M. (2004). The IKK/NF-kappaB activation pathway—a target for prevention and treatment of cancer. *Cancer Lett* **206**: 193–199.
- Grosjean-Raillard J, Ades L, Boehrer S, Tailler M, Fabre C, Braun T *et al.* (2008). Flt3 receptor inhibition reduces constitutive NF-kappaB activation in high-risk myelodysplastic syndrome and acute myeloid leukemia. *Apoptosis* **13**: 1148–1161.
- Guzman ML, Neering SJ, Upchurch D, Grimes B, Howard DS, Rizzieri DA *et al.* (2001). Nuclear factor-kappaB is constitutively activated in primitive human acute myelogenous leukemia cells. *Blood* **98**: 2301–2307.
- Habraken Y, Piette J. (2006). NF-kappaB activation by double-strand breaks. *Biochem Pharmacol* **72**: 1132–1141.
- Halazonetis TD, Gorgoulis VG, Bartek J. (2008). An oncogene-induced DNA damage model for cancer development. *Science* **319**: 1352–1355.
- Hassan Z, Fadeel B, Zhivotovsky B, Hellstrom-Lindberg E. (1999). Two pathways of apoptosis induced with all-trans retinoic acid and etoposide in the myeloid cell line P39. *Exp Hematol* **27**: 1322–1329.
- Hickson I, Zhao Y, Richardson CJ, Green SJ, Martin NM, Orr AI *et al.* (2004). Identification and characterization of a novel and specific inhibitor of the ataxia-telangiectasia mutated kinase ATM. *Cancer Res* **64**: 9152–9159.
- Huang TT, Wuerzberger-Davis SM, Wu ZH, Miyamoto S. (2003). Sequential modification of NEMO/IKKgamma by SUMO-1 and ubiquitin mediates NF-kappaB activation by genotoxic stress. *Cell* **115**: 565–576.
- Janssens S, Tinel A, Lippens S, Tschopp J. (2005). PIDD mediates NF-kappaB activation in response to DNA damage. *Cell* **123**: 1079–1092.
- Karin M, Yamamoto Y, Wang QM. (2004). The IKK NF-kappa B system: a treasure trove for drug development. *Nat Rev Drug Discov* **3**: 17–26.
- Knapper S. (2007). FLT3 inhibition in acute myeloid leukaemia. *Br J Haematol* **138**: 687–699.
- Leone G, Pagano L, Ben-Yehuda D, Voso MT. (2007). Therapy-related leukemia and myelodysplasia: susceptibility and incidence. *Haematologica* **92**: 1389–1398.
- Li N, Banin S, Ouyang H, Li GC, Courtois G, Shiloh Y *et al.* (2001). ATM is required for IkappaB kinase (IKK) activation in response to DNA double strand breaks. *J Biol Chem* **276**: 8898–8903.
- Lin X, Ramamurthi K, Mishima M, Kondo A, Howell SB. (2000a). p53 interacts with the DNA mismatch repair system to modulate the cytotoxicity and mutagenicity of hydrogen peroxide. *Mol Pharmacol* **58**: 1222–1229.
- Lin Y, Ma W, Benchimol S. (2000b). Pidd, a new death-domain-containing protein, is induced by p53 and promotes apoptosis. *Nat Genet* **26**: 122–127.
- Metivier D, Dallaporta B, Zamzami N, Larochette N, Susin SA, Marzo I *et al.* (1998). Cytofluorometric detection of mitochondrial alterations in early CD95/Fas/APO-1-triggered apoptosis of Jurkat T lymphoma cells. Comparison of seven mitochondrion-specific fluorochromes. *Immunol Lett* **61**: 157–163.
- Mufti G, List AF, Gore SD, Ho AY. (2003). Myelodysplastic syndrome. *Hematology Am Soc Hematol Educ Program* **2003**: 176–199.
- Rajkumar SV, Richardson PG, Hideshima T, Anderson KC. (2005). Proteasome inhibition as a novel therapeutic target in human cancer. *J Clin Oncol* **23**: 630–639.
- Tinel A, Tschopp J. (2004). The PIDDosome, a protein complex implicated in activation of caspase-2 in response to genotoxic stress. *Science* **304**: 843–846.
- Vardiman JW, Harris NL, Brunning RD. (2002). The World Health Organization (WHO) classification of the myeloid neoplasms. *Blood* **100**: 2292–2302.
- Wu ZH, Shi Y, Tibbetts RS, Miyamoto S. (2006). Molecular linkage between the kinase ATM and NF-kappaB signaling in response to genotoxic stimuli. *Science* **311**: 1141–1146.
- Yanada M, Matsuo K, Suzuki T, Kiyoi H, Naoe T. (2005). Prognostic significance of FLT3 internal tandem duplication and tyrosine kinase domain mutations for acute myeloid leukemia: a meta-analysis. *Leukemia* **19**: 1345–1349.
- Zamzami N, Kroemer G. (2004). Methods to measure membrane potential and permeability transition in the mitochondria during apoptosis. *Methods Mol Biol* **282**: 103–115.